TISSUE ENGINEERING: Part C Volume 28, Number 7, 2022 © Mary Ann Liebert, Inc. DOI: 10.1089/ten.tec.2022.0102



Open camera or QR reader and scan code to access this article and other resources online.



METHODS ARTICLE

Spatial Recombinant Human Bone Morphogenetic Protein 2 Delivery from Hydroxyapatite Scaffolds Sustains Bone Regeneration in Rabbit Radius

Joo L. Ong, PhD,¹ Stefanie M. Shiels, PhD,^{1,2} Joseph Pearson, PhD,^{1,3} Suyash Karajgar, MS,¹ Solaleh Miar, PhD,¹ Gennifer Chiou, BS,¹ Mark R. Appleford, PhD,¹ Joseph C. Wenke, PhD,^{2,4} and Teja Guda, PhD¹

Regenerating large bone defects requires a multifaceted approach combining optimal scaffold designs with appropriate growth factor delivery. Supraphysiological doses of recombinant human bone morphogenetic protein 2 (rhBMP2), typically used for the regeneration of large bone defects clinically in conjunction with an acellular collagen sponge (ACS), have resulted in many complications. In this study, we develop a hydroxyapatite/ collagen I (HA/Col) scaffold to improve the mechanical properties of the HA scaffolds, while maintaining open connected porosity. Varying rhBMP2 dosages were then delivered from a collagenous periosteal membrane and paired with HA or HA/Col scaffolds to treat critical-sized (15 mm) diaphyseal radial defect in New Zealand white rabbits. The groups examined were ACS +76 μg rhBMP2 (clinically used INFUSE dosage), HA +76 μg rhBMP2, HA +15 µg rhBMP2, HA/Col +15 µg rhBMP2, and HA/Col +15 µg rhBMP2 + bone marrow-derived stromal cells (bMSCs). After 8 weeks of implantation, all regenerated bones were evaluated using microcomputed tomography, histology, histomorphometry, and torsional testing. It was observed that the bone volume regenerated in the HA/Col +15 µg rhBMP2 group was significantly higher than that in the groups with 76 µg rhBMP2. The same scaffold and growth factor combination resulted in the highest bone mineral density of the regenerated bone, and the most bone apposition on the scaffold surface. Both the HA and HA/Col scaffolds paired with 15 µg rhBMP2 had sustained ingrowth of the mineralization front after 2 weeks compared to the groups with 76 µg rhBMP2, which had far greater mineralization in the first 2 weeks after implantation. Complete bridging of the defect site and no significant difference in torsional strength, stiffness, or angle at failure were observed across all groups. No benefit of additional bMSC seeding was observed on any of the quantified metrics, while bone-implant apposition was reduced in the cell-seeded group. This study demonstrated that the controlled spatial delivery of rhBMP2 at the periosteum at significantly lower doses can be used as a strategy to improve bone regeneration around space maintaining scaffolds.

Keywords: bone, hydroxyapatite, collagen, periosteal, rhBMP2

Department of Biomedical Engineering and Chemical Engineering, University of Texas at San Antonio, San Antonio, Texas, USA.

²Combat Wound Care, US Army Institute of Surgical Research, Ft. Sam Houston, San Antonio, Texas, USA.

³Wallace H. Coulter Department of Biomedical Engineering, Georgia Institute of Technology, Atlanta, Georgia, USA. ⁴Department of Orthopedic Surgery and Rehabilitation, University of Texas Medical Branch, Galveston, Texas, USA.

The work was performed at the University of Texas at San Antonio and the U.S. Army Institute of Surgical Research.

Tweet

Inside-out or outside-in: growth factors delivered from the outside of porous mineral-collagen scaffolds, maintain strength and regrow bone better in a rabbit study.

Twitter handle for senior author (@Guda_Lab) and sponsoring institution (@UTSA)

Impact Statement

This study provides insights on bone regeneration in the presence of spatially controlled delivery of recombinant human bone morphogenetic protein 2 (rhBMP2) from porous hydroxyapatite scaffolds coated with collagen I films. Using critical-sized defects created in the radial diaphysis of skeletally mature New Zealand White rabbits, microcomputed tomography and histomorphometry indicated significantly higher bone regeneration, bone mineral density, and bone-implant contact, as well as sustained regeneration over longer durations with lower dosage of rhBMP2 delivered periosteally.

Introduction

ARGE VOLUMETRIC BONE defects that are stabilized, but untreated, do not heal of their own accord. Multiple synthetic biomaterial scaffolds have been developed as bone grafts to treat large bone defects. The focus in such research has primarily been on material osteoconductivity: scaffolds that act to maintain space within the large defect to maintain anatomical form and reduce the local strain to physiological levels, and are readily infiltrated and remodeled by the osteoblasts as they regenerate new bone tissue. Polymeric matrices, ¹⁻³ gels, ⁴⁻⁶ ceramic scaffolds, ^{7,8} and composite ⁹⁻¹³ systems have been widely investigated for bone regeneration, and each system has its own unique advantages and drawbacks. Ceramic scaffolds, especially calcium phosphates, are similar to the native mineral phase of bone, ¹⁴ but are brittle and structural ceramics are difficult to shape to precisely fit bone defects.

Hydroxyapatite (HA) is the synthetic osteoconductive ceramic similar to the mineral in native bone (biological apatite) and can be prepared to have mechanical properties similar to bone tissue. 14 In previous studies, we have shown that porous HA scaffolds (pore sizes ranging from 200 to 500 µm) provided enhanced bone regeneration and mechanical support in segmental defects in vivo. 8,15 Specifically, we designed a bilayer HA scaffold to mimic the cortical and trabecular structure of bone, finding that the flexural toughness was similar to autologous bone grafts that are considered the gold standard treatment.⁸ In another study, we tested the porous HA scaffold paired with a collagen wrap to act both like a barrier membrane as well as a periosteal scaffold to guide bone growth. This approach was shown to increase bone mineral density, regenerated bone volume, and interfacial bone ingrowth.

The porous HA scaffold can also have varying pore sizes, which we recently demonstrated differentially impact scaffold vascularization *in vitro*¹⁷ since the matrix mechanics within pores directs vascular sprouting and growth. In this study, we propose a method to improve the mechanical properties of HA scaffolds by coating the surface of the scaffold with collagen type I, the primary extracellular matrix protein in native bone tissue. In addition to improving mechanical properties, this approach could potentially improve cell attachment and availability of growth factors during bone regeneration.

Bone scaffold materials are usually paired with osteoinductive growth factors to induce osteogenesis. For example, the use of BMP2 and BMP7¹⁸ is clinically approved for the regeneration of large bony defects. However, the recommended dosages of these growth factors for regenerative applications are supraphysiological by several orders of magnitude. These high doses have been associated with exorbitant costs and serious adverse effects, including life-threatening cervical swelling, osteoclast activation with transient bone resorption, ectopic bone formation, and cyst-like bone void formation. P-22 Approaches that allow a reduced dose of BMP2 to be used will allow for greater safety and efficacy in bone regeneration procedures. In this study, we propose that the spatial control of BMP2 can be used to maintain efficacy of regeneration at lower doses. This hypothesis is tested by reducing the BMP2 dose to 20% of clinical dosage, and delivering it periosteally using the same delivery mechanism.

The triad of factors traditionally used to regenerate bone tissue is completed by osteogenic cells. Mesenchymal stem cells (MSCs) are typically recruited endogenously to the site of injury in normal bone regeneration.²³ To ensure both rapid and adequate osteogenic cells locally, the addition of MSCs to the scaffold has been previously tested with mixed results.²⁴ In this study, we test whether the pairing of an optimized hydroxyapatite-collagen I (HA/Col) porous scaffold with the periosteal delivery of rhBMP2 would accelerate bone tissue regeneration in a critical-sized segmental defect in the rabbit radius if supplemented by bone marrowderived MSCs. Compared to control groups, all assessed in the same model for a period of 8 weeks allow the comprehensive evaluation of various osteoconductive, osteoinductive, and osteogenic factors and their relative import in promoting bone tissue regeneration.

Materials and Methods

Scaffold preparation

The HA scaffolds were prepared using a polymer template coating and sintering process as previously described. Briefly, interconnected polyurethane sponges (EN Murray, Denver, CO) with a mean pore size of 340 µm were twice coated with HA slurry, vacuum dried overnight, and sintered at 1230°C for 3 h to allow a 100% crystalline HA structure to be formed and for the underlying polyurethane template to be fully oxidized. The sponge templates were designed to mimic a 15 mm segmental defect in the rabbit radius model and had an elliptical cross-section to match explanted bone, which averaged a 5 mm major axis and a 3 mm minor axis.

To modify these ceramic scaffolds to more closely mimic native bone and to improve mechanical properties, thin film collagen I coatings were applied to the scaffolds. HA scaffolds were coated with a 4% (weight:volume) rat tail collagen I in 0.05M acetic acid solution by immersion and drainage. Immediately, pores in scaffold architecture were exposed through the use of controlled air pressure. Scaffolds were allowed to dry overnight at 37°C, followed by a wash with deionized water. The procedure was repeated to provide scaffolds a second coat of collagen. All scaffolds were sterilized using ethylene oxide gas sterilization before *in vitro* studies or *in vivo* implantation.

Scaffold characterization

The porosity of scaffolds was characterized using helium pycnometry (Accupyc 1340, Norcross, GA)²⁵ to measure the true scaffold solid volume (V_{solid}) for HA scaffolds with and without collagen coating (n=8 samples/group). Microcomputed tomography (microCT) scans were performed using Skyscan 1076 (Skyscan, Kontich, Belgium) at a 8.77 µm pixel resolution and images were reconstructed using Mimics software (v11, Materialise, Leuven, Belgium). The microCT images were thresholded such that the HA scaffold volume from the microCT matched the V_{solid} measured from helium pycnometry, and the low-density material around the scaffold was identified as collagen. Mechanical strength, elastic modulus, and toughness of HA scaffolds with and without collagen coating (n=5 samples/group)were measured by compression to failure (Insight 5, MTS, Eden Prairie, MN) in displacement control mode at a constant strain rate of 0.125 mm/min.²⁵

Human embryonic palatal mesenchymal cells were grown and maintained in Dulbecco's modified Eagle's medium (DMEM) F-12 media supplemented with 10% fetal bovine serum (FBS) and 1% antibiotic/antimycotic mixture. Cells were seeded on scaffolds at 2×10^6 cells/scaffold and cultured for 9 days using osteogenic media (DMEM with 7% FBS, 1% antibiotic-antimycotic, 50 mg/mL L-ascorbic acid, 10^{-8} dexamethasone, and 10 mM β -glycerol phosphate) with medium changes and collection every 2 days. Cell proliferation (by measuring metabolic activity) was assessed using an Alamar Blue assay 26 on days 3, 5, 7, and 9. Commitment to an osteogenic lineage was assessed by measuring alkaline phosphatase (ALP) production in the supernatant media on days 1, 3, 5, 7, and 9. Four samples per time point per group were evaluated for the *in vitro* cell culture.

Animal Model

A unilateral 15 mm critical-sized bone defect was created in the radial diaphysis of skeletally mature New Zealand White rabbits (Myrtles Rabbitry, Inc., Thompson Station, TN). A 25 mm incision was made over the middle third of the radius. The overlying tissues were then dissected to expose the radial diaphysis, where a 15 mm segmental defect was created with an oscillating saw (MicroAire Surgical Instruments, Charlottesville, VA), under saline irrigation. The entire segment of the native radius was removed to create the bony defect, and the periosteum scraped and removed for a 5 mm region from the defect interfaces, but the interosseous syndesmosis (the intact periosteum between the radius and the ulna in rabbits) was left intact.

Following the defect creation, the surgical site was treated with (a) an acellular collagen sponge (ACS) with the recommended 76 μg dose of rhBMP2 (INFUSE®, clinical control) for this model or a 15 mm HA scaffold described previously combined with either a recommended 76 μg rhBMP2 dose or an experimental 15 μg rhBMP2 (20%) dose loaded onto the ACS and wrapped around the scaffold 16 within the defect site. Furthermore, the collagen-coated HA scaffold either (d) without cells or (e) seeded with 2×10^6 rabbit bone marrow MSCs 24 both paired with the 15 μg rhBMP2 dose loaded onto the ACS was evaluated. The MSCs were isolated from bone marrow aspirates from the tibia and iliac crest of donor rabbits as previously reported. 24

Briefly, after aseptic exposure of the tibia and iliac crest using a drill, a 15-gauge aspiration needle was inserted and a syringe containing heparin was used to collect the marrow. Ficoll-Paque addition and centrifugation at 500 g for 10 min were used to first remove the buffy coat layer, followed by washing with phosphate -saline (PBS) containing 2 mM of ethylenediaminetetraacetate and centrifugation two times at 500 g for 10 min. Nucleated cells from this were then seeded in tissue culture flasks and maintained in Minimum Essential Medium Eagle-alpha modification (α -MEM) supplemented with 20% FBS, 1% antibiotic-antimycotic, and 2 mM L-glutamine. Nonadherent cells were removed after 48 h of culture, the adherent cells (considered passage 0) expanded to confluence, and the cells used for *in vivo* studies were within passage 3.

The ACS was stretched around the defect site and held in place by cerclage sutures that were tied around the radius and ulna, both proximal and distal to the defect site. All animals (10 animals per treatment type) were kept alive for 8 weeks postsurgery. The rabbits received sequential fluorochrome labels for calcium at 2 weeks (Calcein green), 4 weeks (xylenol orange), and 6 weeks (tetracycline) following scaffold implantation.²⁴ These labels were used to understand ingrowth at various stages of bone healing within the groups.

The protocol was approved by the Institutional Animal Care and Use Committee at the Army Institute of Surgical Research, Ft. Sam Houston, TX, and followed the Guide for Care and Use of Laboratory Animals. After 8 weeks, animals were euthanized and the radius-ulna complex was excised. From each group, three samples were preserved in formalin for histological evaluation, while the other seven samples were wrapped in PBS-soaked gauze and frozen before mechanical testing. All 10 samples were scanned for microCT evaluation.

MicroCT evaluation

MicroCT analysis of specimen hydrated with PBS or in formalin was performed on Skyscan 1076 (Bruker Corporation, Allentown, PA) at a 8.77 μm pixel resolution as previously described. 8.15,16,24 Briefly, the total bone formed within the defect site (region of interest) was measured, based on differences in density. New bone evaluation was conducted by distinguishing "density ranges in Houndsfield Units (HU)" between the scaffold (HU: 1080–3050), native bone (HU: 740–1080) and the newly forming osteoid or remodeling native bone (HU: 200–740). The mineralized tissue volume was separated based on location into the volume occupied by the scaffold and surrounding bone, which

was labeled as callus to distinguish spatial bone regeneration patterns. The region of interest evaluated included the 15 mm defect span. The bone mineral density of the regenerated ossified tissue in the defect space was also calculated for all samples to assess the quality of bone regeneration. ^{2,23}

Histological evaluation

Bone-scaffold blocks were embedded in photo-curing resin (Exakt 7200 VLC, Oklahoma City, OK), and thin sections of the bone-scaffold blocks were prepared using a precision microsaw. The sections were stained with Paragon (Multiple Tissue Stain) and Aniline Blue, which stains collagen/bone blue and vessels/soft tissue pink, and imaged. Prepared slides were imaged for polyfluorochrome stains using specific filters (excitation/emission wavelengths: L5 480/527 nm, N3 546/600 nm, Chroma 425/475LP nm) as previously described. Image channels were then merged to create composite 2-, 4-, and 6-week bone fronts in the red/blue/green channels with an additional layer for phase-contrast imaging of the final bone front at 8 weeks.

Bone front measurements and all histomorphometry analysis were performed on high-resolution images using BioquantOsteo (Nashville, TN). The basic measurements were distance between the bone fronts, then summed and averaged to determine depth of infiltration, the bone area inside scaffold, and bone-scaffold contact length as a percentage of scaffold perimeter.

Biomechanical evaluation

The seven samples/groups were thawed from frozen and kept constantly hydrated using PBS throughout the torsional testing protocol. The distal ends of the antebrachial sections were embedded in Loctite marine epoxy and allowed to cure for 24 h on each end. Once fully cured, the ulna was removed from the load transfer by cutting through the distal ends without disturbing the interosseous membrane. The samples were loaded horizontally into a TG160 torsion machine (TestResources Inc., Shakopee, MN). The functional mechanical evaluation was conducted at a constant torsional strain rate of 1°/sec until failure (50% drop in load). Torsional modulus, strength, maximal angle at failure, and torsional toughness were measured and normalized to the uninjured contralateral limb, which was also tested in an identical manner.

Statistical Analysis

All data are reported as mean \pm standard error of the mean. Statistical significance of the changes in porosity and mechanical properties due to collagen coating on HA scaffolds; and statistical differences in the *ex vivo* groups measured by microCT, torsional testing, and histomorphometry were determined using one-way analysis of variance (ANOVA) followed by Tukey's *post-hoc* test. Significant differences for the *in vitro* evaluation (across time and collagen coating) as well as the *in vivo* evaluation of bone infiltration measures (across time and scaffold group) reported were determined using a two-way ANOVA and Tukey's test for *post-hoc* evaluation. Any statistical test with p < 0.05 was deemed significant, and all statistical testing was conducted using SigmaStat (v14.5, Inpixion, Palo Alto, CA).

Results

Scaffold characterization

An open pore structure with uniform collagen coating was observed by microCT imaging of HA scaffolds (Fig. 1A). The porosity and mechanical characterization of HA scaffolds (Table 1) without and with a thin film coating of rat tail Collagen I (HA/Col) demonstrated a small reduction (but significant, $p\!=\!0.019$) in porosity from $88.01\pm0.66\%$ to $85.76\pm0.53\%$, but increased compressive strength significantly by $149\pm16\%$ ($p\!<\!0.001$). The toughness of scaffolds, which is the amount of energy that can be absorbed before failure, also increased significantly by $363\pm122\%$ ($p\!=\!0.042$).

During compressive testing to failure, no macrodamage or collapse of the scaffolds was observed of the collagen-coated HA scaffolds, while the uncoated HA scaffolds have a fracture plane usually at 450 and evident breakage of scaffold struts until the scaffold structure itself collapses (Fig. 1B). Alamar blue-based quantification of cell activity (Fig. 1C) indicated significant increase in both HA and HA/Col scaffolds over time (p < 0.0001), with the activity in the HA/Col group being significantly higher as a main effect (p < 0.0001). ALP quantification in the supernatant media (Fig. 1D) showed the characteristic significant increase (p < 0.0001) at time points after 3 days of *in vitro* culture with osteogenic media, but no impact of collagen coating on the scaffolds was observed (p = 0.163).

MicroCT evaluation

The 15 mm critical-sized defect created in the rabbit radius was restored with one of five groups (1) ACS +76 μg rhBMP2, (2) HA +76 μg rhBMP2, (3) HA +15 μg rhBMP2, (4) HA/Col +15 μg rhBMP2, and (5) HA/Col +15 μg rhBMP2 + MSCs and evaluated 8 weeks after implantation (Fig. 2). MicroCT reconstructions showed bridging across the critical-sized 15 mm gap in all groups evaluated and integration of the bone ingrowth within the pores of the scaffolds in the HA and HA/Col scaffold groups (Fig. 3A). The inclusion of the ACS membrane as a periosteal graft showed distinct ossification in the scaffold groups in the region surrounding the bone defect and contributed to the mineralized callus in the volumetric quantification.

In the rabbit radius model, three distinct fronts of bone ingrowth are observed: from the proximal and distal interfaces of the defect site as well as from the ossification of the interosseous syndesmosis between the radius and ulna that exist in rabbits (Fig. 3A). In the case of the ACS +76 µg rhBMP2, since no scaffold was present to maintain space, some soft tissue impingement resulted in the regenerated bone tissue in the defect occupying less space than the radius bone defect site (concave shape longitudinally instead of the native convex curvature is observed in Fig. 3A). No fragmentation of the scaffolds included was observed and the structure of the HA and HA/Col scaffolds was retained at 8 weeks (Supplementary Fig. S1), and as anticipated, much denser than the regenerated bone.

Regenerated bone volume was quantified within the 15 mm defect span and the bone volume regenerated in the HA/Col +15 μ g rhBMP2 group (497 \pm 46 mm³) was significantly higher than the bone volume in the ACS +76 μ g

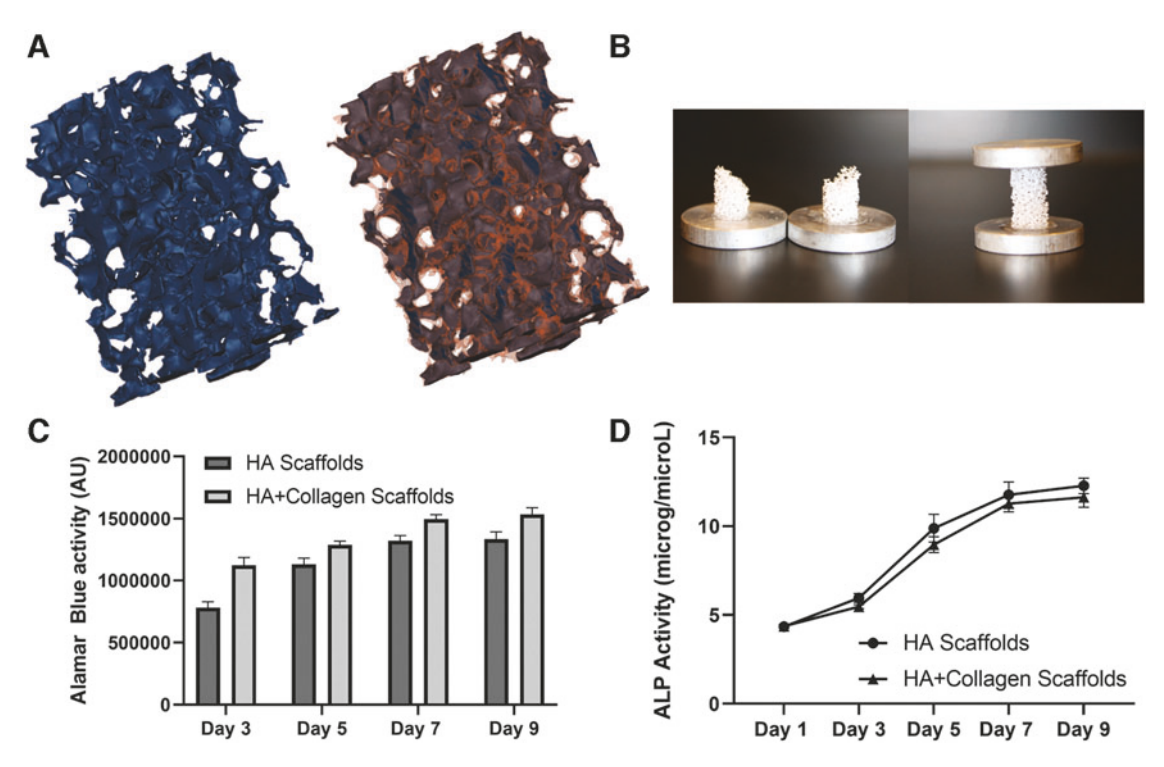


FIG. 1. HA Scaffold characterization after collagen coating. (**A**) MicroCT reconstruction of a $2 \times 2 \times 4$ mm block of the HA scaffold (pseudo colored *blue*) without and after collagen (pseudo color *orange*) coating. (**B**) Compressive testing of HA scaffolds without collagen coating (*left*) showing shear failure, while after collagen coating did not show macroscale failure damage. (**C**) Alamar blue cellular activity on scaffolds demonstrated a significant increase with time (p < 0.0001) and a significant increase with collagen coating across time (p < 0.0001). (**D**) Significant increase in alkaline phosphatase activity (p < 0.0001) observed with time across both groups with no impact of collagen coating. HA, hydroxyapatite; microCT, microcomputed tomography.

rhBMP2 and HA +76 μ g rhBMP2 groups (p=0.015, Fig. 3B). This difference in regenerated bone between groups was consistent at various depths along the proximal to distal 15 mm defect span, with the HA/Col +15 μ g rhBMP2 group containing significantly greater bone area within the defect (Supplementary Fig. S2), and across groups, the proximal bone growth front was more prominent than the distal front. No significant difference was found in the overall bone volume regenerated with the addition of MSCs to the HA/Col +15 μ g rhBMP2 group (452 \pm 29 mm³, p=0.87).

The mineral density of the regenerated bone was quantified as a metric of bone quality (Fig. 3C) and was highest in the HA/Col +15 μ g rhBMP2 group (1.12 \pm 0.04 mgHA/cm³), which was significantly greater than the bone mineral density of the regenerated bone in the HA +76 μ g rhBMP2 scaffolds (0.89 \pm 0.06 mgHA/cm³, p=0.004). The bone mineral density was not significantly different between the other treatment groups.

Histological evaluation

Histological evaluation of the bone regenerated within the scaffolds and the ACS group with rhBMP2 supported the observations from the microCT images. Mineralized collagenous tissue was observed in the periosteal region of all defects after 8 weeks, especially at the sites where the ACS had been placed around the scaffolds (Fig. 4A). The fraction of available defect area filled with new bone area was calculated and was found to be highest in the HA/Col +15 μ g rhBMP2 scaffolds (34.6±2.9%), which was significantly greater than the bone area fraction of the regenerated bone in the ACS +76 μ g rhBMP2 group (22.4±5.1%, p=0.015, Fig. 4B).

Since the engraftment of the biomaterial scaffolds is dependent on the contact between the newly regenerated bone with the scaffold surface, the percentage of scaffold surface in direct contact with new bone perimeter was

Table 1. Changes in the Porosity and Mechanical Properties of Hydroxyapatite Scaffolds After Collagen Coating

	HA	HA + Col	Increase (%)	p
Porosity (%)	88.01 ± 0.66	85.76±0.53	-2.55 ± 0.60^{a}	0.019
Strength (MPa)	0.38 ± 0.09	0.95 ± 0.06	149.1 ± 16.1^{a}	< 0.001
Stiffness (MPa)	90.1 ± 16.4	107.6 ± 6.0	19.4 ± 6.6	0.309
Toughness (MPa)	0.87 ± 0.45	4.04 ± 1.07	362.7 ± 122.2^{a}	0.042

^aSignificant differences and the corresponding *p*-value. Col, collagen I; HA, hydroxyapatite.

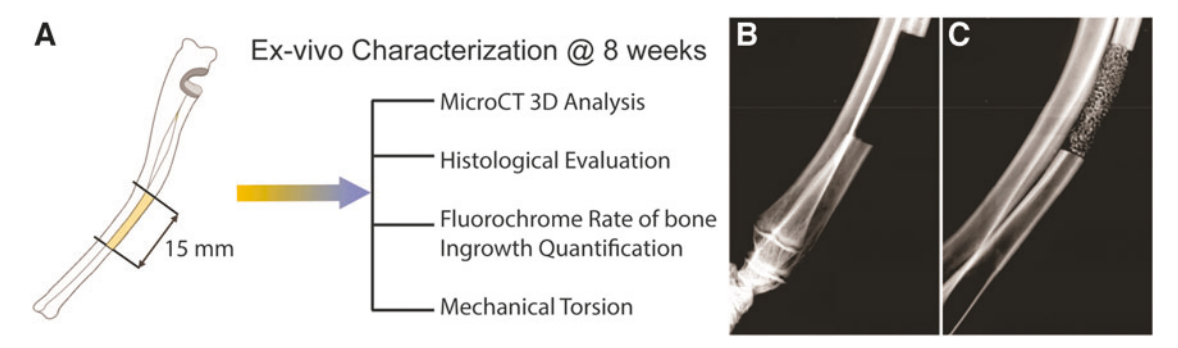


FIG. 2. Critical-sized rabbit radius model. **(A)** A 15 mm defect in the rabbit radius is naturally supported by the ulna and does not need additional fixation. The defect was restored with one of five groups (1) ACS +76 μg rhBMP2, (2) HA +76 μg rhBMP2, (3) HA +15 μg rhBMP2, (4) HA/Col +15 μg rhBMP2, and (5) HA/Col +15 μg rhBMP2 + MSCs and evaluated 8 weeks after implantation. **(B)** Treatment with the ACS sponge and the collagen wrap is not visible in postsurgery radiographs, while **(C)** the HA scaffold used to treat the defect site is radio-opaque immediately after placement. ACS, acellular collagen sponge; Col, collagen I; MSC, mesenchymal stem cells; rhBMP2, recombinant human bone morphogenetic protein 2.

quantified for the four treatments, which included the HA and HA/Col scaffolds. While bone was observed in direct apposition on the surface of both the HA and HA/Col scaffolds (average Bone/Scaffold contact $30.8\pm3.2\%$), cellular debris was found between the new bone tissue and the scaffold surface in the HA/Col +15 µg rhBMP2 + MSC group (Bone/Scaffold contact $14.9\pm1.9\%$, p=0.17, Fig. 4C).

Fluorochrome labeling

Sequential fluorochrome injection (calcein green, xylenol orange, and tetracycline) labels were used to stain mineral deposition at 2, 4, and 6 weeks after implantation to indicate progression of bone regeneration within the defect (Fig. 5A). The extent of bone mineral fronts was calculated

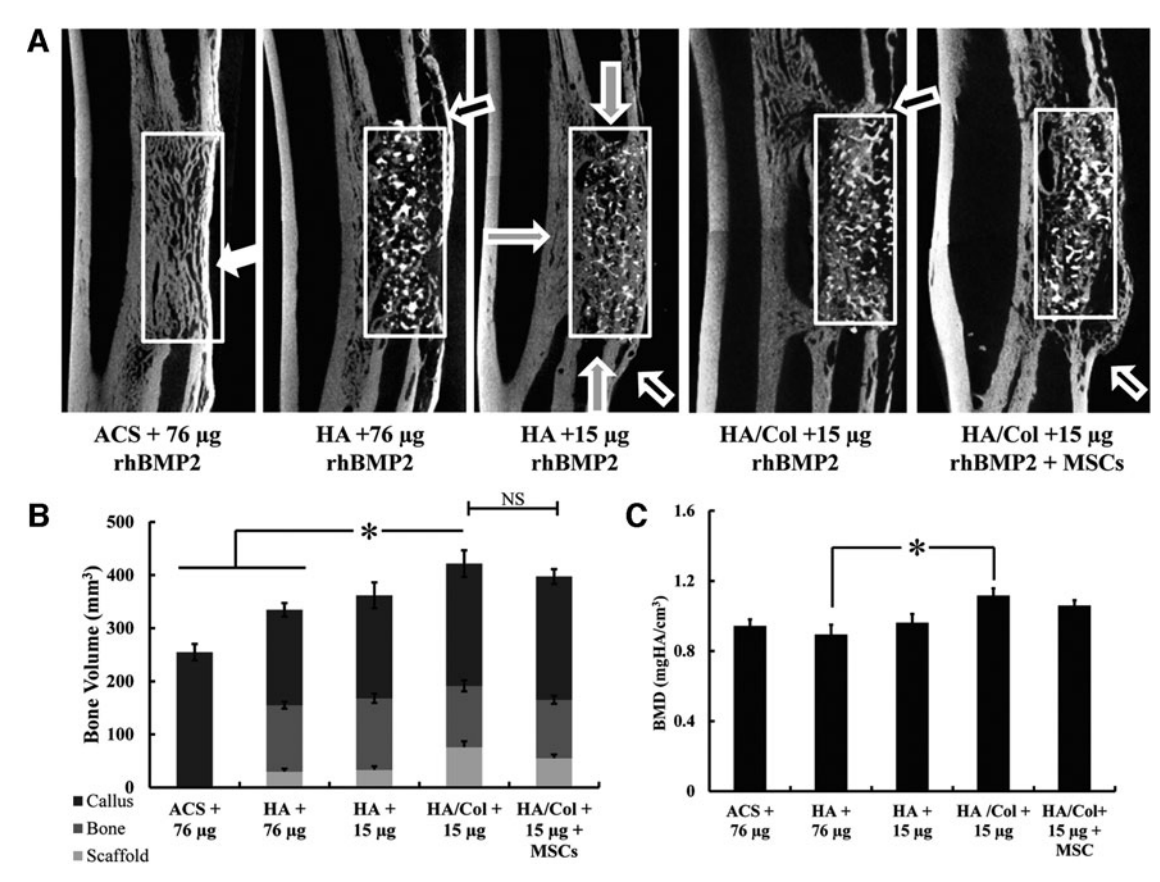


FIG. 3. MicroCT characterization after 8 weeks. **(A)** Longitudinal representative microCT sections of the defect site 8 weeks after implantation (*white* shows poor space maintenance, *black arrows* show stabilizing callus, and *gray arrows* indicate bone fronts). **(B)** Bone volume measurements showed that ACS +76 μg rhBMP2 regenerated the least bone, while the HA/Col scaffolds with 15 μg of rhBMP2 regenerated greater mineralized tissue than the ACS and HA scaffolds at 76 μg of rhBMP2 (indicated by *). **(C)** These results also supported the bone mineral density evaluation, indicating regenerated bone quality.

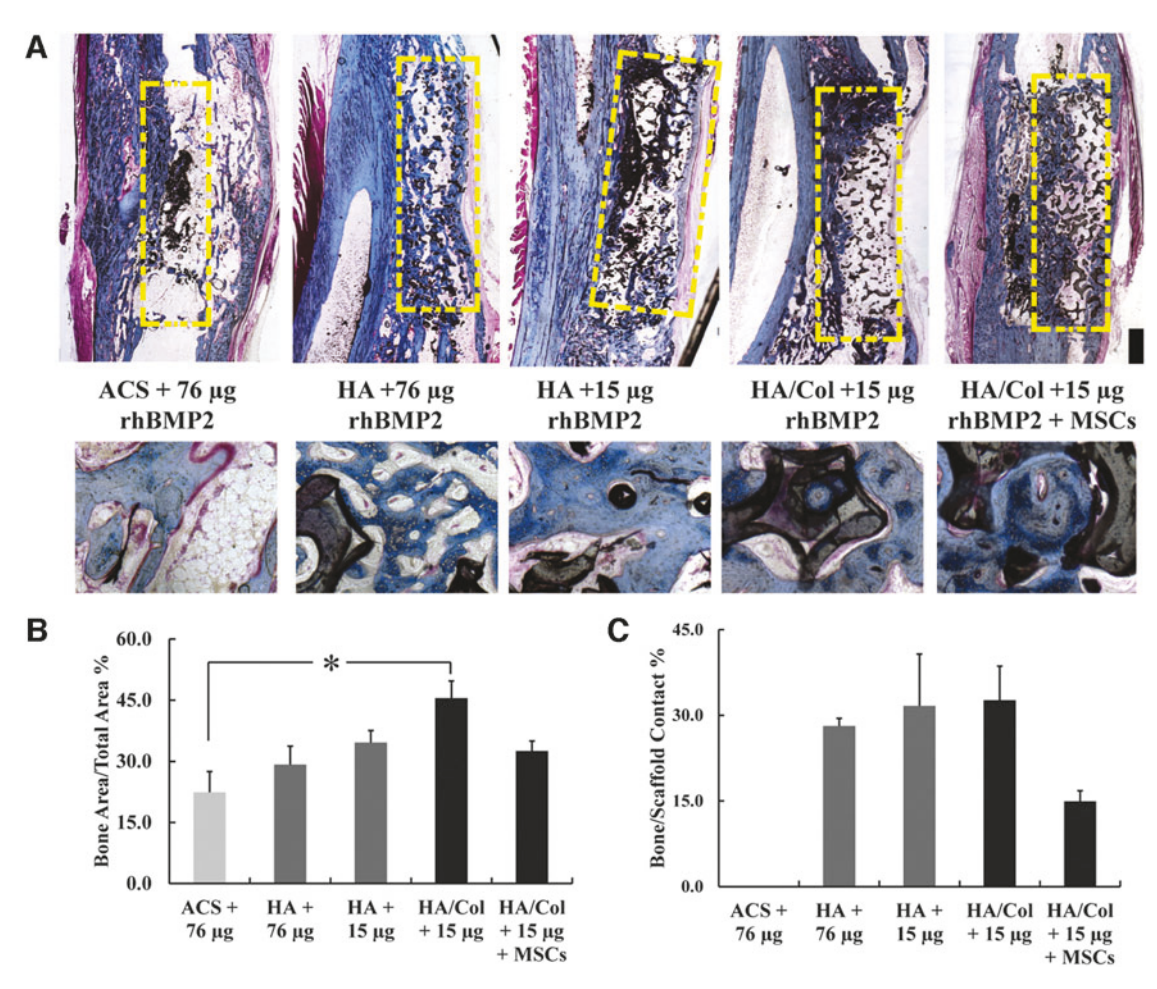


FIG. 4. Histomorphometric analysis of the bone regeneration. (**A**) Histological sections stained with Paragon (*Pink*) for soft tissues, Aniline *Blue* (*Blue*) for mineralized tissue. Scaffold is *black* ($4 \times$ magnification composite images). *Inset* images show the apposition of bone tissue against the scaffold (*black*) at $20 \times$ magnification. (**B**) Bone area measurement indicated that the collagen-coated HA scaffold with 15 µg of rhBMP2 regenerated greater mineralized tissue than the ACS with 76 µg of rhBMP2 (shown by *), (**C**) Percentage bone/scaffold contact using stained histological sections (significant differences shown by *, p < 0.05).

independently from the proximal and distal interfaces as well as from the interosseous syndesmosis with the ulna, but only the net sum of infiltration from the proximal and distal defect margins is reported for each of the five treatments after the first 2 weeks, from week 2 to 4, and from week 4 to 6.

In the groups with the $76\,\mu g$ rhBMP2 (both with ACS and HA scaffolds), a majority of the bone infiltration was observed in the first 2 weeks ($75.4\pm9.9\%$ of total in growth) compared to the three groups with $15\,\mu g$ rhBMP2, where only $38.1\pm5.3\%$ of total in growth happened over the first 2 weeks. In distinct contrast, in the groups with $15\,\mu g$ rhBMP2, continued robust bone regeneration progression over weeks 2–4 was observed ($60.4\pm5.1\%$ of total in growth) compared to only $22.1\pm9.4\%$ further in the groups with $76\,\mu g$ rhBMP2. The overall bone regeneration progression observed in weeks 2–4 was significantly greater in the HA/Col +15 μg rhBMP2 group ($3191\pm462\,\mu m$, p=0.035) compared to the ACS + $76\,\mu g$ rhBMP2 ($318\pm60\,\mu m$) and HA + $76\,\mu g$ rhBMP2 ($315\pm253\,\mu m$) during the same time (Fig. 5B).

Biomechanical testing

Functional torsional testing of the radii was conducted to failure for all five groups. Since there is a high variability between animals irrespective of treatment groups in the absolute values of torsional strength and stiffness, contralateral radii were used to normalize results and reduce interanimal variations (Table 2). In terms of absolute values, the torsional stiffness was found to be highest in the HA/Col +15 μg rhBMP2 group (60±16 N.mm/deg) compared to 41±13 N.mm/deg for the ACS +76 μg rhBMP2 treatment.

No significant difference was observed in torsional stiffness, maximal torque loading, maximal angle at failure, and torsional toughness between any of the treatments. The HA +15 μ g treatment showed highest torque (130 \pm 26% of contralateral), torsional stiffness (229 \pm 101% of contralateral), and overall toughness (140 \pm 21% of contralateral), whereas the ACS +76 μ g demonstrated the greatest angular rotation (155 \pm 41% of contralateral) recovery at break (Table 2, Supplementary Fig. S3).

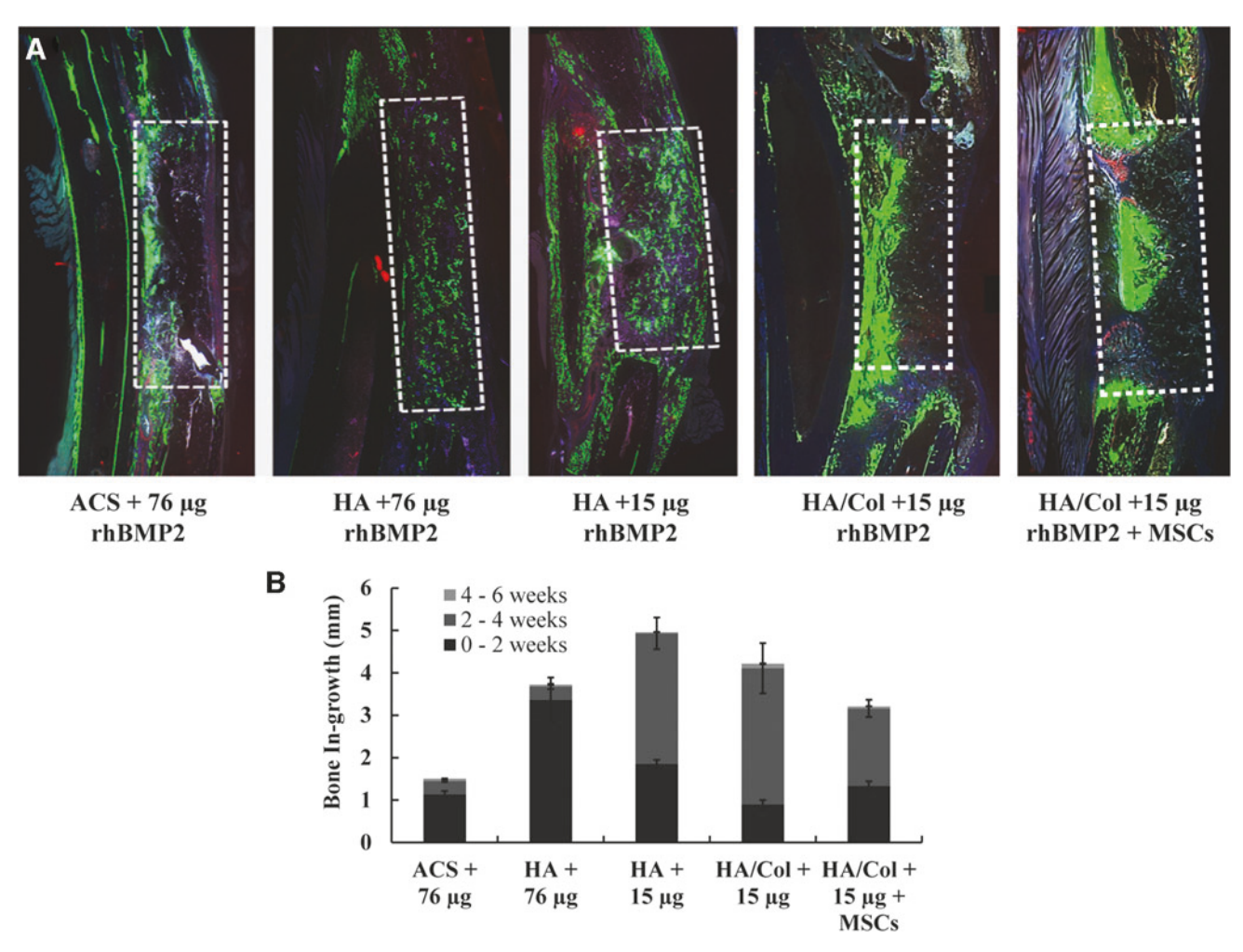


FIG. 5. Quantifying the rate of bone infiltration. (**A**) Fluorochrome injections of Calcein *Green* (false *green*) at 2 weeks, Xylenol *Orange* (false *red*) at 4 weeks, and Tetracycline (false *blue*) at 6 weeks indicate progression of bone regeneration within defect. Diffused bone fronts are observed within the scaffold groups. (**B**) The rate of bone infiltration after 2, 4, and 6 weeks across all groups indicates that HA with 76 μg rhBMP2 after first 2 weeks, while HA/Col scaffolds without MSCs show greater bone regeneration in the 2–4-week time frame compared to the 0–2- and the 4–6-week time frames.

Discussion

Porous HA scaffolds function as efficient space maintaining constructs that provide a Ca²⁺ source for bone regeneration, but do not show significant degradation or loss of structure over time.²⁷ Conversely, a majority of collagen-HA based systems previously investigated have actually been based on porous collagen scaffolds coated with nano-HA^{28,29} or incorporating microparticles of HA.^{13,30,31}

The nano-HA coatings are usually deposited using ${\rm Ca}^{2+}$ and ${\rm PO_4}^{3-}$ ion-rich fluids such as simulated body fluids and

are intended to rapidly provide these same ions to promote an osteogenic response.³² The microparticles of HA act both as the porogens within the collagen matrices, which open up pores for bone regeneration^{30,33} upon being resorbed by wound site macrophages when implanted,³⁴ and provide the additional benefit when incorporated into the collagenous scaffolds to noncovalently bind³⁵ to and increase bioavailability of growth factors such as BMP2 and vascular endothelial growth factor,³⁶ which promote regeneration of vascularized bone. These collagen-HA scaffolds are highly porous (>95%), but the structural porosity is

TABLE 2. TORSIONAL MECHANICAL PROPERTIES OF THE SURGICALLY RESTORED RADII COMPARED TO THEIR CONTRALATERAL RADII FOR EACH OF THE TREATMENT GROUPS

	Max torque (%)	Stiffness (%)	Max angle (%)	Torsional toughness (%)
ACS+76 μg	113.1 ± 18.7	151.1 ± 29.5	155.1 ± 41.0	107.5 ± 29.0
HA +76 μg	102.8 ± 14.4	192.8 ± 29.4	114.5 ± 25.7	70.3 ± 9.3
HA +15 μg	130.0 ± 26.2	229.3 ± 101.2	107.3 ± 13.4	139.9 ± 21.4
HA/Col +15 μg	107.7 ± 17.4	181.9 ± 21.9	67.7 ± 6.9	99.3 ± 22.6
$HA/Col + 15 \mu g + MSCs$	78.4 ± 10.6	93.8 ± 10.9	90.6 ± 15.2	88.4 ± 21.8

MSC, mesenchymal stem cells.

between proteinaceous collagen sheets (prepared by acid dissolution and lyophilization) and/or created by particles of calcium phosphate.

Since the overall modulus of these scaffolds is very low (0.2–4 kPa), ^{34,37} they can be infiltrated and remodeled easily by cells and mineralized tissue. The strategy to promote bone regeneration using HA and HA/Col scaffolds developed in this study is diametrically different. Specifically, the porosity of HA scaffolds is open, interconnected porosity (85–88%) organized by large (12- to 14- sided polyhedral) pores closely packed to result in open windows between pores. When coated with thin films of collagen I, by dip coating and vacuum evacuation, the porosity only showed a minor reduction, while the strength improved to 0.95 MPa and elastic modulus to 107 MPa (Table 1).

Similar preparations of HA scaffolds by template coating, then further coated by collagen I and vacuum evacuation, have been reported previously, but resulted in much lower porosity, as well as poor mechanical properties (fracture strength <0.3 MPa, modulus <8 MPa).³⁸ Thus, the HA/Col scaffolds developed in this study were significantly tougher and unlike the uncoated HA scaffolds, did not show brittle fracture either in mechanical testing (Fig. 1) or in microCT observations around the HA scaffold edges sometimes observed after *in vivo* implantation.¹⁵

While the traditional triad of bone tissue engineering has revolved around osteoconductive scaffolds, osteogenic cells, and osteoinductive growth factors, it has been well documented that the biomechanical stability^{39,40} and effective mechanotransduction at the defect site²³ are equally critical to maintain continued bone regeneration. The use of ACS as wraps to protect the microenvironment of the defect site and provide mechanical protection from micromotion have been demonstrated previously by our group in both the rat femoral defect with internal fixation,⁴¹ as well as the rabbit radius model without additional fixation.¹⁶ The ACS, by virtue of the location it is placed in, functions as a *de facto* periosteal scaffold. Previous work has attempted to rely on the use of the periosteum to provide instructive cues toward the development of novel biomaterials capable of regenerating vascularized bone in the defect sites.⁴²

Specifically, the periosteum is known to be richly populated by both capillary endothelial cells and pericytes⁴³ and can contribute to vascularization and osteogenesis within bone grafts. We found that the use of collagen-guided membranes in long bone defects resulted in increased control of the regenerative microenvironment and enhanced osteoconductivity of bone scaffolds, primarily through the formation of a stabilizing callus, ¹⁶ which was observed in the microCT, and histological analyses of this study as well.

While guided membranes have been used extensively for craniofacial applications, 44 it is only recently 45 that they are being recognized as potential mechanisms to harness a native periosteum-mimicking response. The secondary advantage of using the collagenous membrane as a periosteal guide is the ability to leverage it to deliver growth factors effectively at the defect site. ACS is the clinically approved carrier for rhBMP2 (as the INFUSE product by Medtronic, which forms the ACS +76 µg rhBMP2 group in this study).

However the rapid, bolus release from the ACS, and associated concerns with local inflammation and sequelae, has been widely documented in literature. 46,47 While the mea-

sured concentration of BMP2 is $\sim 21.4\pm12\,\text{ng/g}$ from demineralized bone obtained from human donors, clinical treatment of fractures currently uses a supraphysiological dose of $800,000\,\text{ng/mL}$. Although the approved delivery of supraphysiological doses of BMPs has shown considerable promise in treating critical-sized bone defects when compared to autografts, limitations to such use include high associated costs, upregulation of BMP inhibitors such as noggin, and the adverse effects that are sometimes life threatening. ¹⁸

The supraphysiological doses are buffered by pairing the ACS + rhBMP2 with calcium phosphates, which bind the rhBMP2^{47,49} and increase duration of local availability. However, the early burst of rhBMP2 has been credited to function more as an endogenous osteogenic progenitor recruitment signal to the site of injury, while a sustained release of rhBMP2 acts as a strong differentiation signal. ^{1,6} In the rabbit radius model, for a critical-sized defect, the clinical-equivalent recommended dose is 70–75 μ g of rhBMP2, ^{50,51} while there have been multiple studies evaluating lower doses. ^{52–54} Results in this study, in terms of the torsional mechanical properties (Table 2) as well as the bone volume regenerated in the HA/Col +15 μ g rhBMP2 group (Fig. 3), are comparable or significantly higher than these reports. This is likely due to both the dose and location of the rhBMP2 delivery.

The ACS-based periosteal delivery of rhBMP2 as an early bolus sets up an external chemotactic gradient, and is effective at low doses since it targets recruitment of endogenous cells, and rapidly forms an ossified callus, which further creates a protected microenvironment and increases defect site stability. The same ACS-based delivery within the defect site is buffered by the HA and results in prolonged mineralization (between weeks 2 and 4 in this study, Fig. 5) and osteogenesis within the scaffold. This buffering within the scaffold is potentially greater in the case of the HA/Col scaffold, explaining the trend of greater bone volume and mineral density observed in that group compared to the HA scaffolds at the same 15 µg rhBMP2 dose.

Osteogenic cells are critical to ensuring bone regeneration within critical-sized defects. MSCs can be harvested autologously from the patient for seeding the graft, and are known to be both osteogenic as well as immunomodulatory. Theoretically, the addition of MSCs to the fracture site should lead to more successful unions. However, the results on that front have been mixed. In previous studies, we demonstrated that HA scaffolds with or without undifferentiated MSCs in two seeding densities, implanted in the rabbit radius, regenerated the same bone volume after 4 weeks.

Furthermore, in the same study, 8 weeks after implantation, the scaffold with no MSCs actually regenerated more bone volume than the cell-seeded groups. ²⁴ Possible explanations for this observation are that the absence of MSC seeding promoted a more robust recruitment response, that the early autocrine signaling mechanism of MSCs was triggered with a suboptimal population density, or that *in situ* recruited cells show superior callus formation. However, a lack of cell seeding and being restricted to endogenous recruitment can also be a limitation.

In the porous HA scaffolds ($350\,\mu m$ pore size) implanted in $10\,mm$ segmental bone defects in the rabbit radius, a significant proximal to distal interface bias in regeneration was observed. This was attributed to compromised vascular supply at the distal end, which led to limited tissue infiltration

in the scaffold interior. 16 This lack of vasculature is hypothesized to impede the regeneration of bone across large defects in the extremities and craniofacial skeleton, 56 leading to the concept of "critical size bone defects," which do not heal of their own accord. In this study, $\sim 11,300/\text{mm}^3$ rabbit bone marrow MSCs were seeded on the HA/Col scaffolds and paired with 15 μg rhBMP2 on the ACS periosteally. That group performed no different in terms of bone volume, mineral density, and torsional properties as the group with the HA/Col scaffold and 15 μg rhBMP2, but no cell seeding.

This is contrary to findings of significant improvements in bone regeneration reported in mouse models, both of subcutaneous ($\sim\!4000/\text{mm}^3$ human adipose-derived stem cells⁵⁸) implantation as well as calvarial orthotopic defect ($\sim\!200,\!000/\text{mm}^3$ donor MSCs⁵⁹) implantation on collagen-HA scaffolds in immunocompromised animals. One potential hypothesis to explain these differences (in addition to the immune-competent vs. immune-compromised animal models) is that the survival of implanted MSCs is determined by the local vascularization or lack thereof. In mouse calvarial models, a net scaffold thickness of 500 $\mu\text{m}^{59,60}$ ensures that seeded cells, even at extremely high densities, are not far removed from the vasculature. The high cell seeding density also does not compete with endogenous recruitment in the calvarial model since the local soft tissue volume adjacent to the defect that would be a source of endogenous recruitment is fairly limited.

In the ectopic subcutaneous pouch, there is far greater vasculature and soft tissue surrounding the site, but the cell seeding density employed was relatively low. Histological observations from the HA/Col +15 µg rhBMP2 + MSCs group in this study clearly indicated lower bone apposition-scaffold contact because of cellular debris on the scaffold surface, which was not observed in any of the other groups (Fig. 4). So, in addition to the MSCs actually reducing endogenous recruitment after the initial inflammatory response, it is likely that implanted cell death due to lack of sufficiently rapid vascularization further reduced any additional benefit from seeding MSCs.

We recently demonstrated the ability to maintain viable osteogenic and angiogenic *in vitro* cell cultures by pairing MSC seeding on the HA scaffolds with adipose tissuederived microvascular fragments within the pores of the scaffolds. Future success of MSC seeding on scaffolds may require prevascularization of the graft to ensure rapid inosculation to host vasculature so as to provide the necessary nutrients for MSC survival.

Conclusions

In this study, we demonstrate that coating open porous HA scaffolds with a thin film of collagen I significantly improves mechanical strength and toughness without noticeable change in porosity. We then demonstrate in a critical-sized defect in the rabbit radius that pairing the HA/Col scaffolds with 20% of the recommended rhBMP2 dose when delivered periosteally using a collagen membrane results in far greater bone volume regenerated, and improved bone mineral density, bone-scaffold contact and torsional strength. Moreover, in this study, the additional implantation of MSCs on these scaffolds did not improve bone regeneration. The HA/Col scaffolds thus offer a viable design to function as effective space maintainers to promote bone regeneration.

Authors' Contributions

J.L.O.: conceptualization, methodology, writing, and funding acquisition. S.M.S. and S.K.: methodology, investigation, and data curation. J.P.: methodology, investigation, data curation, and writing. S.M. and G.C.: formal analysis, visualization, and writing. M.R.A.: methodology and visualization. J.C.W.: conceptualization, project administration, and writing. T.G.: conceptualization, methodology, investigation, data curation, writing, and supervision.

Disclaimer

The views expressed in this article are those of the authors and do not reflect the official policy or position of the U.S. Army Medical Department, Department of the Army, DoD, or the U.S. Government.

Ethics Approval

Research was conducted in compliance with the Animal Welfare Act, the implementing Animal Welfare regulations, and the principles of the Guide for the Care and Use of Laboratory Animals, National Research Council. The facility's Institutional Animal Care and Use Committee approved all research conducted in this study. The facility where this research was conducted is fully accredited by AAALAC.

Disclosure Statement

No competing financial interests exist.

Funding Information

This study was supported, in part, by the Orthopaedic Extremity Trauma Research Program No. W81XWH-08-1-0393 of the U.S. Department of Defense. S.M. and T.G. were also supported by the Oak Ridge Institute for Science and Education, and T.G. was supported, in part, by funding from the National Science Foundation (CBET Award 1847103).

Supplementary Material

Supplementary Figure S1 Supplementary Figure S2 Supplementary Figure S3

References

- Brown KV, Li B, Guda T, et al. Improving bone formation in a rat femur segmental defect by controlling bone morphogenetic protein-2 release. Tissue Eng Part A 2011;17(13–14): 1735–1746; doi: 10.1089/ten.TEA.2010.0446.
- Guda T, Darr A, Silliman DT, et al. Methods to analyze bone regenerative response to different rhBMP-2 doses in rabbit craniofacial defects. Tissue Eng Part C Methods 2014;20(9):749–760; doi: 10.1089/ten.TEC.2013.0581.
- Shah AR, Cornejo A, Guda T, et al. Differentiated adiposederived stem cell cocultures for bone regeneration in polymer scaffolds in vivo. J Craniofac Surg 2014;25(4): 1504–1509; doi: 10.1097/scs.0000000000000755.
- Boerckel JD, Kolambkar YM, Dupont KM, et al. Effects of protein dose and delivery system on BMP-mediated bone regeneration. Biomaterials 2011;32(22):5241–5251; doi: 10 .1016/j.biomaterials.2011.03.063.

- Kim S, Bedigrew K, Guda T, et al. Novel osteoinductive photo-cross-linkable chitosan-lactide-fibrinogen hydrogels enhance bone regeneration in critical size segmental bone defects. Acta Biomater 2014;10(12):5021–5033; doi: 10 .1016/j.actbio.2014.08.028.
- 6. Kolambkar YM, Boerckel JD, Dupont KM, *et al.* Spatiotemporal delivery of bone morphogenetic protein enhances functional repair of segmental bone defects. Bone 2011;49(3):485–492; doi: 10.1016/j.bone.2011.05.010.
- Stubbs D, Deakin M, Chapman-Sheath P, et al. In vivo evaluation of resorbable bone graft substitutes in a rabbit tibial defect model. Biomaterials 2004;25(20):5037–5044; doi: 10.1016/j.biomaterials.2004.02.014.
- 8. Guda T, Walker JA, Pollot BE, *et al.* In vivo performance of bilayer hydroxyapatite scaffolds for bone tissue regeneration in the rabbit radius. J Mater Sci Mater Med 2011;22(3):647–656; doi: 10.1007/s10856-011-4241-7.
- Chesnutt BM, Viano AM, Yuan Y, et al. Design and characterization of a novel chitosan/nanocrystalline calcium phosphate composite scaffold for bone regeneration. J Biomed Mater Res A 2009;88(2):491–502; doi: 10.1002/ jbm.a.31878.
- Dadsetan M, Guda T, Runge MB, et al. Effect of calcium phosphate coating and rhBMP-2 on bone regeneration in rabbit calvaria using poly(propylene fumarate) scaffolds. Acta Biomater 2015;18:9–20; doi: 10.1016/j.actbio.2014.12.024.
- Dias GJ, Mahoney P, Swain M, et al. Keratinhydroxyapatite composites: biocompatibility, osseointegration, and physical properties in an ovine model. J Biomed Mater Res A 2010;95(4):1084–1095; doi: 10.1002/ jbm.a.32908.
- 12. Schek RM, Wilke EN, Hollister SJ, *et al.* Combined use of designed scaffolds and adenoviral gene therapy for skeletal tissue engineering. Biomaterials 2006;27(7):1160–1166; doi: 10.1016/j.biomaterials.2005.07.029.
- Wahl DA, Czernuszka JT. Collagen-hydroxyapatite composites for hard tissue repair. Eur Cell Mater 2006;11:43–56; doi: 10.22203/eCM.v011a06.
- 14. Guda T, Appleford M, Oh S, *et al.* A cellular perspective to bioceramic scaffolds for bone tissue engineering: the state of the art. Curr Top Med Chem 2008;8(4):290–299; doi: 10.2174/156802608783790956.
- 15. Guda T, Walker JA, Singleton B, *et al.* Hydroxyapatite scaffold pore architecture effects in large bone defects in vivo. J Biomater Appl 2014;28(7):1016–1027; doi: 10.1177/0885328213491790.
- Guda T, Walker JA, Singleton BM, et al. Guided bone regeneration in long-bone defects with a structural hydroxyapatite graft and collagen membrane. Tissue Eng Part A 2013;19(17–18):1879–1888; doi: 10.1089/ten.TEA.2012.0057.
- 17. Chiou G, Jui E, Rhea AC, *et al.* Scaffold architecture and matrix strain modulate mesenchymal cell and microvascular growth and development in a time dependent manner. Cell Mol Bioeng 2020;13(5):507–526; doi: 10.1007/s12195-020-00648-7.
- 18. Garrison KR, Shemilt I, Donell S, *et al.* Bone morphogenetic protein (BMP) for fracture healing in adults. Cochrane Database Syst Rev 2010;(6):CD006950; doi: 10.1002/14651858.CD006950.pub2.
- 19. Axelrad T, Steen B, Lowenberg D, *et al.* Heterotopic ossification after the use of commercially available recombinant human bone morphogenetic proteins in four patients. J Bone Joint Surg Br 2008;90(12):1617–1622; doi: 10.1302/0301-620X.90B12.20975.

- Nauth A, Giannoudis PV, Einhorn TA, et al. Growth factors: beyond bone morphogenetic proteins. J Orthop Trauma 2010;24(9):543–546; doi: 10.1097/BOT.0b013e3181ec4833.
- Perri B, Cooper M, Lauryssen C, et al. Adverse swelling associated with use of rh-BMP-2 in anterior cervical discectomy and fusion: a case study. Spine J 2007;7(2):235–239; doi: 10.1016/j.spinee.2006.04.010.
- 22. Zara JN, Siu RK, Zhang X, *et al.* High doses of bone morphogenetic protein 2 induce structurally abnormal bone and inflammation in vivo. Tissue Eng Part A 2011; 17(9–10):1389–1399; doi: 10.1089/ten.tea.2010.0555.
- 23. Guda T, Labella C, Chan R, *et al.* Quality of bone healing: perspectives and assessment techniques. Wound Repair Regen 2014;22 Suppl 1:39–49; doi: 10.1111/wrr.12167.
- 24. Rathbone C, Guda T, Singleton B, *et al.* Effect of cell-seeded hydroxyapatite scaffolds on rabbit radius bone regeneration. J Biomed Mater Res Part A 2014;102(5): 1458–1466; doi: 10.1002/jbm.a.34834.
- Guda T, Oh S, Appleford MR, et al. Bilayer hydroxyapatite scaffolds for maxillofacial bone tissue engineering. Int J Oral Maxillofac Implants 2012;27(2):288–294. PMID: 22442766.
- Montelongo SA, Chiou G, Ong JL, et al. Development of bioinks for 3D printing microporous, sintered calcium phosphate scaffolds. J Mater Sci Mater Med 2021;32(8):94; doi: 10.1007/s10856-021-06569-9.
- 27. Appleford MR, Oh S, Oh N, *et al.* In vivo study on hydroxyapatite scaffolds with trabecular architecture for bone repair. J Biomed Mater Res A 2009;89(4):1019–1027; doi: 10.1002/jbm.a.32049.
- 28. Lickorish D, Ramshaw JAM, Werkmeister JA, *et al.* Collagen–hydroxyapatite composite prepared by biomimetic process. J Biomed Mater Res Part A 2004;68A(1):19–27; doi: https://doi.org/10.1002/jbm.a.20031.
- Rodrigues SC, Salgado CL, Sahu A, et al. Preparation and characterization of collagen-nanohydroxyapatite biocomposite scaffolds by cryogelation method for bone tissue engineering applications. J Biomed Mater Res Part A 2013;101A(4): 1080–1094; doi: https://doi.org/10.1002/jbm.a.34394.
- 30. Rodrigues CVM, Serricella P, Linhares ABR, *et al.* Characterization of a bovine collagen–hydroxyapatite composite scaffold for bone tissue engineering. Biomaterials 2003; 24(27):4987–4997; doi: https://doi.org/10.1016/S0142-9612(03)00410-1.
- 31. Wahl DA, Sachlos E, Liu C, *et al.* Controlling the processing of collagen-hydroxyapatite scaffolds for bone tissue engineering. J Mater Sci Mater Med 2007;18(2):201–209; doi: 10.1007/s10856-006-0682-9.
- 32. Boller LA, Shiels SM, Florian DC, *et al.* Effects of nanocrystalline hydroxyapatite concentration and skeletal site on bone and cartilage formation in rats. Acta Biomaterialia 2021;130:485–496; doi: https://doi.org/10.1016/j.actbio.2021.05.056.
- 33. Dumas JE, Prieto EM, Zienkiewicz KJ, *et al.* Balancing the rates of new bone formation and polymer degradation enhances healing of weight-bearing allograft/polyurethane composites in rabbit femoral defects. Tissue Eng Part A 2013;20(1–2):115–129; doi: 10.1089/ten.tea.2012.0762.
- 34. Sridharan R, Genoud KJ, Kelly DJ, *et al.* Hydroxyapatite particle shape and size influence MSC osteogenesis by directing the macrophage phenotype in collagenhydroxyapatite scaffolds. ACS Appl Bio Mater 2020;3(11): 7562–7574; doi: 10.1021/acsabm.0c00801.
- 35. Quinlan E, Thompson EM, Matsiko A, *et al.* Long-term controlled delivery of rhBMP-2 from collagen—

hydroxyapatite scaffolds for superior bone tissue regeneration. J Control Release 2015;207:112–119; doi: https://doi.org/10.1016/j.jconrel.2015.03.028.

- 36. Walsh DP, Raftery RM, Chen G, *et al.* Rapid healing of a critical-sized bone defect using a collagen-hydroxyapatite scaffold to facilitate low dose, combinatorial growth factor delivery. J Tissue Eng Regen Med 2019;13(10):1843–1853; doi: https://doi.org/10.1002/term.2934.
- 37. Al-Munajjed AA, Plunkett NA, Gleeson JP, *et al.* Development of a biomimetic collagen-hydroxyapatite scaffold for bone tissue engineering using a SBF immersion technique. J Biomed Mater Res B Appl Biomater 2009; 90B(2):584–591; doi: https://doi.org/10.1002/jbm.b.31320.
- 38. Islam MS, Todo M. Effects of sintering temperature on the compressive mechanical properties of collagen/hydroxyapatite composite scaffolds for bone tissue engineering. Mater Lett 2016;173:231–234; doi: https://doi.org/10.1016/j.matlet.2016.03.028.
- 39. Giannoudis PV, Einhorn TA, Marsh D. Fracture healing: the diamond concept. Injury 2007;38:S3–S6; doi: 10.1016/S0020-1383(08)70003-2.
- Giannoudis PV, Einhorn TA, Schmidmaier G, et al. The diamond concept-open questions. Injury 2008;39:S5–S8; doi: 10.1016/S0020-1383(08)70010-X.
- 41. Miar S, Pearson J, Montelongo S, *et al.* Regeneration enhanced in critical-sized bone defects using bone-specific extracellular matrix protein. J Biomed Mater Res B Appl Biomater 2021;109(4):538–547; doi: 10.1002/jbm.b.34722.
- 42. Lin Z, Fateh A, Salem DM, *et al.* Periosteum: biology and applications in craniofacial bone regeneration. J Dental Res 2014;93(2):109–116; doi: 10.1177/0022034513506445.
- 43. Pilia M, McDaniel JS, Guda T, *et al.* Transplantation and perfusion of microvascular fragments in a rodent model of volumetric muscle loss injury. Eur Cell Mater 2014;28: 11–23; discussion 23–24; doi: 10.22203/ecm.v028a02.
- 44. Dupoirieux L, Pourquier D, Picot M, *et al.* Comparative study of three different membranes for guided bone regeneration of rat cranial defects. Int J Oral Maxillofac Surg 2001;30(1):58–62; doi: 10.1054/ijom.2000.0011.
- 45. Allan B, Ruan R, Landao-Bassonga E, *et al.* Collagen membrane for guided bone regeneration in dental and orthopedic applications. Tissue Eng Part A 2020;27(5–6): 372–381; doi: 10.1089/ten.tea.2020.0140.
- 46. Kowalczewski CJ, Tombyln S, Wasnick DC, *et al.* Reduction of ectopic bone growth in critically-sized rat mandible defects by delivery of rhBMP-2 from kerateine biomaterials. Biomaterials 2014;35(10):3220–3228; doi: https://doi.org/10.1016/j.biomaterials.2013.12.087.
- 47. Luangphakdy V, Shinohara K, Pan H, *et al.* Evaluation of rhBMP-2/collagen/TCP-HA bone graft with and without bone marrow cells in the canine femoral multi defect model. Eur Cell Mater 2015;29:57–68; doi: 10.22203/eCM.v029a05.
- 48. Pietrzak WS, Woodell-May J, McDonald N. Assay of bone morphogenetic protein-2, -4, and -7 in human demineralized bone matrix. J Craniofac Surg 2006;17(1):84–90; doi: 10.1097/01.scs.0000179745.91165.73.
- Murphy CM, Schindeler A, Gleeson JP, et al. A collagenhydroxyapatite scaffold allows for binding and co-delivery of recombinant bone morphogenetic proteins and bisphosphonates. Acta Biomaterialia 2014;10(5):2250–2258; doi: https://doi.org/10.1016/j.actbio.2014.01.016.
- 50. Pekkarinen T, Jämsä T, Määttä M, et al. Reindeer BMP extract in the healing of critical-size bone defects in the

- radius of the rabbit. Acta Orthop 2006;77(6):952–959; doi: 10.1080/17453670610013286.
- Wheeler DL, Chamberland DL, Schmitt JM, et al. Radiomorphometry and biomechanical assessment of recombinant human bone morphogenetic protein 2 and polymer in rabbit radius ostectomy model. J Biomed Mater Res 1998;43(4):365–373; doi: https://doi.org/10.1002/(SICI)1097-4636(199824)43:4 <365::AID-JBM4>3.0.CO; 2–6.
- 52. El-Ghannam A, Cunningham Jr L, Pienkowski D, *et al.* Bone engineering of the rabbit ulna. J Oral Maxillofac Surg 2007;65(8):1495–1502; doi: 10.1016/j.joms.2006.10.031.
- Kim J, McBride S, Donovan A, et al. Tyrosine-derived polycarbonate scaffolds for bone regeneration in a rabbit radius critical-size defect model. Biomed Mater 2015; 10(3):035001; doi: 10.1088/1748-6041/10/3/035001.
- 54. Wu Y, Hou J, Yin M, *et al.* Enhanced healing of rabbit segmental radius defects with surface-coated calcium phosphate cement/bone morphogenetic protein-2 scaffolds. Mat Sci Eng C 2014;44:326–335; doi: 10.1016/j.msec.2014.08.020.
- 55. Kagami H, Agata H, Tojo A. Bone marrow stromal cells (bone marrow-derived multipotent mesenchymal stromal cells) for bone tissue engineering: Basic science to clinical translation. Int J Biochem Cell Biol 2011;43(3):286–289; doi: https://doi.org/10.1016/j.biocel.2010.12.006.
- Meijer GJ, de Bruijn JD, Koole R, et al. Cell based bone tissue engineering in jaw defects. Biomaterials 2008; 29(21):3053–3061; doi: http://dx.doi.org/10.1016/j.biomate rials.2008.03.012.
- Schmitz JP, Hollinger JO. The critical size defect as an experimental model for craniomandibulofacial nonunions. Clin Orthop Relat Res 1986;205:299–308; doi: 10.1097/ 00003086-198604000-00036.
- 58. Calabrese G, Giuffrida R, Forte S, *et al.* Human adiposederived mesenchymal stem cells seeded into a collagenhydroxyapatite scaffold promote bone augmentation after implantation in the mouse. Sci Rep 2017;7(1):7110; doi: 10.1038/s41598-017-07672-0.
- 59. Villa MM, Wang L, Huang J, *et al.* Bone tissue engineering with a collagen–hydroxyapatite scaffold and culture expanded bone marrow stromal cells. J Biomed Mater Res B Appl Biomater 2015;103(2):243–253; doi: https://doi.org/10.1002/jbm.b.33225.
- 60. Villa MM, Wang L, Rowe DW, *et al.* Effects of cell-attachment and extracellular matrix on bone formation in vivo in collagen-hydroxyapatite scaffolds. PLoS One 2014;9(10):e109568; doi: 10.1371/journal.pone.0109568.

E-mail: teja.guda@utsa.edu

Received: May 13, 2022 Accepted: May 24, 2022 Online Publication Date: July 8, 2022